

## Research paper

## Predicting drug-drug interactions: A deep learning approach with GCN-based collaborative filtering

Yeon Uk Jeong <sup>a</sup>, Jeongwhan Choi <sup>b</sup>, Noseong Park <sup>a,c</sup>, Jae Yong Ryu <sup>a,d</sup>, Yi Rang Kim <sup>a,e</sup>,\*<sup>a</sup> Oncocross Co. Ltd., #905, C Block, Beobwon-ro 11-gil, Songpa-gu, Seoul, 05836, Republic of Korea<sup>b</sup> Department of Artificial Intelligence, Yonsei University, 50 Yonsei-ro, Seodaemun-gu, Seoul, 03722, Republic of Korea<sup>c</sup> School of Computing, Korea Advanced Institute of Science and Technology, 291 Daehak-ro, Yuseong-gu, Daejeon, 34141, Republic of Korea<sup>d</sup> School of Systems Biomedical Science, Soongsil University, Sangdo-ro 369, Dongjak-gu, Seoul, 06978, Republic of Korea<sup>e</sup> Department of Regulatory Science, Kyung Hee University, 26, Kyungheeda-ro, Dongdaemun-gu, Seoul, 02447, Republic of Korea

## ARTICLE INFO

Dataset link: <https://github.com/yeonuk-Jeong/DDI-OCF>

## Keywords:

Drug-drug interactions

Side effect

Graph convolutional network

Collaborative filtering

## ABSTRACT

The use of combination drugs among patients is increasing due to effectiveness compared to monotherapies. However, healthcare providers should continue to be concerned about the potential risks associated with patient safety arising from drug-drug interactions (DDIs) when they use combination drugs. Whereas direct physicochemical interactions contribute to certain cases of DDIs, the majority of DDIs occur because one drug modulates enzymes, such as cytochrome P450, responsible for metabolizing another drug. Therefore, drugs that interact with the same family drugs are more likely to interact with each other by mediating specific enzymes. Adapted from techniques used to recommend users with similar interests, we introduce an AI recommendation model with graph convolutional network (GCN) and collaborative filtering that analyzes the connectivity of interacting drugs rather than their chemical structures. This approach deviates from typical classification models by not requiring sampling of undefined interactions as negative samples, allowing the prediction of potential interactions for all unknown drug pairs, circumventing the challenges associated with selecting negative interactions and data imbalance. Our methodology used the DrugBank database (version 5.1.9 released on January 3, 2022), encompassing 4,072 drugs and 1,391,790 drug pairs with interactions. Furthermore, the robustness of the model was verified through a 5-fold validation and external data validation using TWOSIDES data. Notably, our model's efficacy is established solely through the exploitation of DDI reports, offering a versatile framework capable of accurately predicting interactions among diverse drug types. The source code for this project is distributed on GitHub (<https://github.com/yeonuk-Jeong/DDI-OCF>).

## 1. Introduction

Drug-drug interactions (DDIs) mean that when two or more drugs are administered, their interaction cause a phenomenon that does not occur when each drug is administered alone. DDIs can occur through a variety of mechanisms, making it difficult to conduct a comprehensive investigation in the form of investigating a specific mechanism. According to a report by the Centers for Disease Control and Prevention, one-third of adults in their 60s and 70s in the United States have used five or more prescription drugs [1]. As the number of approved drugs continues to increase, the probability of DDIs correspondingly escalates [2]. As a result, healthcare providers should be more concerned with managing DDIs.

Although the occurrence of DDIs must eventually be demonstrated experimentally or clinically, it is difficult for biologists or clinicians to perform random experiments using all drug combinations in a time- and

cost-effective manner [3]. Therefore, the development of computational methods to solve the problem of identifying DDIs is particularly important to reduce time and cost of experimental proofs. Researchers have proposed a variety of prediction models for DDIs [4,5]. Traditionally, classification models based on the similarity of drug structures have been studied [6–9]. In addition to the structural information of drugs, classification models that reflect the transcriptome information when the drug is treated with cells also show high performance in recent years [10,11]. Research on the application of matrix factorization (MF), the basic concept of recommendation models, has also been advanced through the use of a DDIs network [12–14]. Deep learning and network analysis techniques have been proposed to improve performance by embedding nodes from bioinformatics knowledge networks, but the module that predicts interactions solves as a classification problem using the fully connected layer last [15,16]. The most recent studies

\* Corresponding author at: Oncocross Co. Ltd., #905, C Block, Beobwon-ro 11-gil, Songpa-gu, Seoul, 05836, Republic of Korea.  
E-mail address: [99yirang@oncocross.com](mailto:99yirang@oncocross.com) (Y.R. Kim).

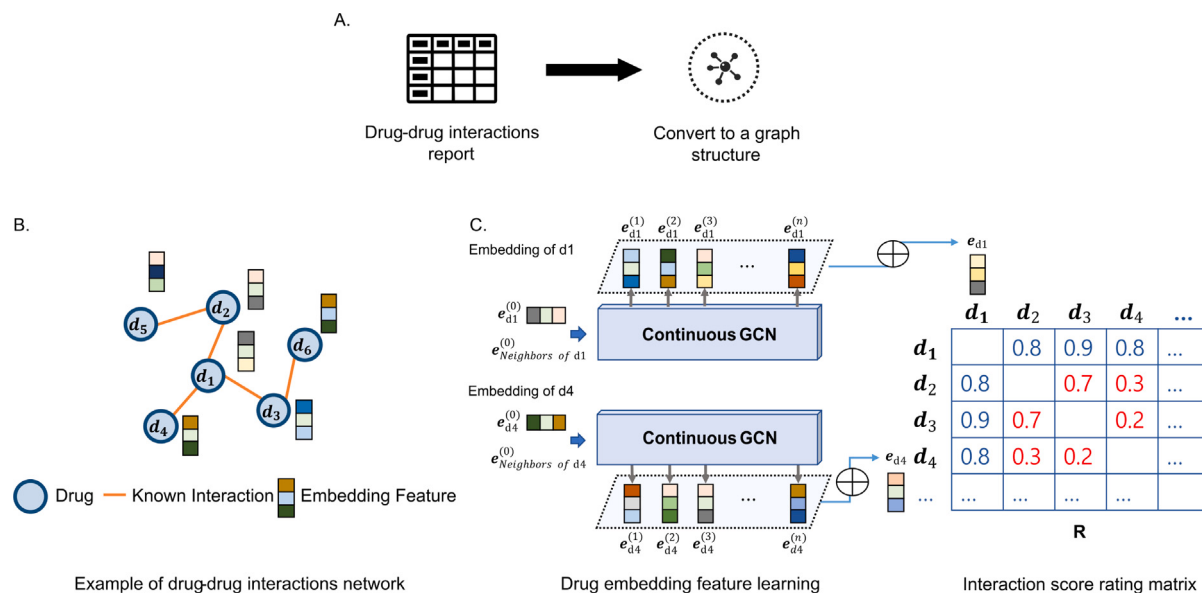


**Fig. 1.** The figure presents the brief composition for the DDIs network and structure of DDIs recommendation model. A: Data from DDIs are reconstructed into a graph structure with nodes and edges. B: An example of a DDIs network. Each node represents a drug, and edges represent known interactions. Each node is described by a trainable embedding feature. C: Schematic representation of training our recommendation model. Refer to Table 1 for notations in the figure. (For interpretation of the references to color in this figure legend, the reader is referred to the web version of this article.)

that defined the molecular structure of a drug in the form of a graph and embedded the drug in a graph convolutional network (GCN) to predict DDIs [17–20]. Also, Yu et al. used GCN to embed features in drug-disease-gene networks and used a MF based predictor, but it also works as a classification model [21]. To overcome the problem that generating random negative samples to train a classification model leads to false negative samples for unobserved facts, interactive network-based learning has been proposed [22].

In contrast with previous papers on the prediction of DDIs, we introduce a recommendation system for the prediction of DDIs. Because the total number of possible combinations between drugs is more than 10 times greater than known DDIs, DDIs data show huge imbalance. In the classification model for predicting the interaction of given two drugs, there is a problem of selecting negative interaction samples, and the model is highly affected by a random seed. Moreover, classification model is more likely to predict no interaction for negative sampling data that has already been used for training. To avoid these problems, we introduced a model to learn the entire network structure of DDIs and predict new interactions. Furthermore, even in papers published in the 2020s, the data sets used in the DDI prediction model had less than 700 [8,9,11,12,14,15,20] and approximately 2000 drugs or fewer [7,10,13,16,18,19,21]. In comparison, 4072 drugs and 1,391,790 drug pair with interactions were used in this study by preprocessing DrugBank data [23] and the interactions were divided into 6:4 for training and test. Lastly, TWOSIDES, a database of only small molecules, was used to compare the performance with and without structural information. Using a report of DDIs information exclusively, an equivalent level of prediction performance was obtained when incorporating structural details. It can simplify the analysis of a wide range of drugs, including biologics. We distributed our model named 'DDI-OCF' as an open source project via GitHub to make it more accessible and transparent.

## 2. Materials and methods

This section presents an introduction to our experimental environments, data preprocessing and model building. The software and hardware environments used for the experiments are as follows: Ubuntu 18.04 LTS, Python 3.7.9, Numpy 1.19.5, Scipy 1.5.2, PyTorch 1.7.1, torchdiffeq 0.2.0, CUDA 11.2, NVIDIA Driver 460.56 and NVIDIA Quadro RTX 8000.

**Table 1**  
Notations used in this paper.

Symbol	Description
$d_i$	Drug $i$
$e_{di}^{(n)}$	Embedding of drug $i$ at $n$ th obtained by ODE
$E_d$	Final drug embedding matrix
$e_{di}$	Final drug embedding of drug $i$
$R$	Interaction score rating matrix
$A$	Interaction matrix (Adjacency matrix)

Note:  $i$  and  $n \in \mathbb{N}$ ,  $\mathbb{N} = \{1, 2, 3, \dots, \infty\}$ .

### 2.1. Drug-drug interactions datasets

In this study, we collected data sets from real-world data and constructed the DDIs network from the DrugBank and TWOSIDES (Table 2). DrugBank<sup>1</sup> version 5.1.9, released on January 3, 2022, was used. The TWOSIDES data were obtained from BioSNAP, and BioSNAP is a collection of publicly available data related to social networks and graph analysis in biology [24]. In the original DDIs data from DrugBank, the number of drugs is 4437 and the number of drug combinations with reported interactions is 1,392,791. This is the number of drug combinations reported as having an interaction, which does not take into account the type of interaction. These data were organized into a graph of nodes and edges, where each node represents a drug, and each edge represents an interaction.

The number of possible drug combinations in the real-world is vast, but combinations with known interactions are relatively sparse. Density means the ratio of the number of drug combinations that actually have any interactions to the number of all possible drug combinations (Table 2). TWOSIDES has a high density of 15.26% because it collects highly interacting drugs, but the DrugBank containing more than 4000 drugs has a low density of 8.39%. If any of the drugs has only very few connections, they may be inadequate for training and evaluation. For this reason, drugs with fewer than 5 connections to other drugs were removed. Finally, 4072 drugs, 1,391,790 interactions were selected. The TWOSIDES data set is used all data without removing drugs with

<sup>1</sup> <https://go.drugbank.com>.

**Table 2**  
Details of datasets after preprocessing.

Datasets	No. of drugs	Interactions	Density
DrugBank(ver. 5.1.9)	4072	1,391,790	8.39%
TWOSIDES	645	63,473	15.26%

fewer connections due to the small number of data. It consists of 645 drugs and 63,473 drug combinations with interactions. The data set is divided 6:4 into a training set and a test set based on the number of edges. Each partitioned set forms a single graph, with no isolated nodes. To demonstrate the robustness of the model, a 5-fold validation was conducted. The DrugBank data contain 1,391,790 interactions, divided into five parts, each consisting of 278,358 interactions. Each distinct validation subgraph has drug counts of 4053, 4047, 4047, 4047 and 4052 respectively.

## 2.2. Recommendation model of drug-drug interactions

**Fig. 1** shows the overall scheme of how DDI-OCF works. Initially, the DDIs data were transformed into a graph structure, with drugs represented as nodes and interactions as edges (**Fig. 1A**). Each drug possesses its own distinctive embedding feature (**Fig. 1B**). Subsequently, these embedding features are updated during the model training process. The GCN learns the interaction relationships between drugs and updates the drug node features. Applying the trained features to the collaborative filtering (CF) technique provides a ranking of the likelihood of interaction for all other drugs (**Fig. 1C**). Feature information is collected based on spatial graph convolution, and the trainable-time ODE (ordinary differential equation) has the effect of going through multiple convolution layers. The model produces a final embedding  $\mathbf{e}_{di}$  for a particular drug by weighted summation of all the computed intermediate embeddings (eg.,  $\mathbf{e}_{di}^{(n)}$ ). After training, the dot product of the features for each drug will finally represent the probability of its association  $\mathbf{E}_d \mathbf{E}_d^\top = \mathbf{R}$ . The numbers in the interaction score rating matrix  $\mathbf{R}$  in **Fig. 1** are examples, with red indicating newly predicted interactions. The interaction score rating matrix  $\mathbf{R}$  is trained to assign elevated scores to drugs associated with known interactions, as well as to assign high scores to potential interactions that have yet to be discovered. We applied LT-OCF [25], an improved version of LightGCN [26] that brings parameter reduction and performance improvements to the recommendation model. In contrast to other traditional GCN-based methods, LT-OCF uses continuous layers by using any positive real number  $t$  that is trainable. The basic idea behind GCN is to aggregate the features of neighboring nodes through iterative graph convolution and combine them into a new representation of the target node [26]. We define the number of drugs  $N$  and the interaction matrix, also known as the adjacency matrix,  $\mathbf{A} \in \{0, 1\}^{N \times N}$  representing the association of DDIs is defined as follows.  $A_{u,i}$  is 1 if an interaction between drugs  $u$  and  $i$  is observed, and 0 otherwise. Also, we introduce self-loops in the interaction matrix to ensure that the model continues to represent the drug's own features as it undergoes graph convolution. Thus, the matrix is  $A_{i,i} = 1$ . To normalize the interaction matrix, we denote the diagonal matrix by  $\mathbf{D} = \text{Diag}(\mathbf{A} \cdot \mathbf{1})$ . The normalized interaction matrix is denoted as  $\tilde{\mathbf{A}} = \mathbf{D}^{-\frac{1}{2}} \mathbf{A} \mathbf{D}^{-\frac{1}{2}}$ . Each node has a feature vector representing a drug, and the model trains the drug feature vector so that the final feature vector of each drug can be filtered through dot product calculation. Our continuous GCN layer updates the embedding matrix for the entire drug and the model trains to reduce error by comparing the dot product of the final drug embedding with the actual interaction. The training process for drug feature embedding vector can be written as follows:

$$\mathbf{E}^{(1)} = \mathbf{E}^{(0)} + \int_0^{t_1} f(\mathbf{E}(t)) dt,$$

$$\begin{aligned} \mathbf{E}^{(2)} &= \mathbf{E}^{(1)} + \int_{t_1}^{t_2} f(\mathbf{E}(t)) dt, \\ &\vdots \\ \mathbf{E}^{(n)} &= \mathbf{E}^{(n-1)} + \int_{t_{n-1}}^{t_n} f(\mathbf{E}(t)) dt \end{aligned} \quad (1)$$

where  $f(\cdot)$  is a linear GCN,  $f(\mathbf{E}(t)) := \frac{d\mathbf{E}(t)}{dt} = \tilde{\mathbf{A}}\mathbf{E}(t)$ . We note that the matrix of the drug feature embedding is  $\mathbf{E}(t) \in \mathbb{R}^{N \times M}$ , where  $N$  is the number of drugs and  $M$  is the size of the embedding, at several different trainable time points  $t \in \{t_1, \dots, t_n\}$ ,  $t \in \mathbb{R}$ , where  $n$  is a hyperparameter, and  $0 < t_{n-1} < t_n$ . A range of solvers can be used to calculate ODEs, which have demonstrated the ability to generalize neural network architectures [27,28]. It is acknowledged that the fourth-order Runge–Kutta (RK4) ODE solver resembles both dense convolutional networks and fractal neural networks [29], and we adapted it. It was compared to Euler, another representative solver, and RK4 slightly outperformed. In Eq. (1), the term preceding the integral component means residual connection, which incorporates the previous embedding. In our implemented code, the option is provided to enable or disable this residual connection. Since self-loops have already been introduced into the interaction matrix, there was no significant difference in the metric without enabling this option.

The final drug embedding matrix  $\mathbf{E}_d \in \mathbb{R}^{N \times M}$  is calculated as follows:

$$\mathbf{E}_d = w_0 \mathbf{E}^{(0)} + \sum_{i=1}^n w_i \mathbf{E}^{(i)}. \quad (2)$$

The model can add each embedding matrix according to a fixed ratio of  $w_i$ . In this paper, our model has the same ratio and  $w_0, w_i$  is all 1. From the dot product of the final drug embedding matrix, we can infer new interactions in the entire drug graph. The interaction score rating matrix  $\mathbf{R} \in \mathbb{R}^{N \times N}$  is calculated from the dot product of the final drug embedding matrix  $\mathbf{E}_d$ .  $\mathbf{R}$  is trained to assign elevated scores to drugs associated with known interactions, as well as to assign high scores to potential interactions that have yet to be established.

## 2.3. Evaluation metrics

To evaluate the performance, precision@K and recall@K were calculated. Precision@K and recall@K are metrics of how well a recommendation system performs when making K recommendations (refer to **Fig. 2**). For example, for a given drug A, the recommendation system may suggest K drugs that it predicts will interact with drug A. If there are 5 drugs that actually interact with drug A, and 3 drugs match the K recommendations, then precision@K is defined as 3/K and recall@K is defined as 3/5. DDI-OCF recommends drugs that may have interactions with the given drugs in the test set, but does not recommend interactions that have already been trained in the training set. For evaluation, the DDIs divided by 6:4 to use as training/test set and implement 5-fold cross validation (CV) to prove robustness our model.

## 2.4. Objective function

For training DDI-OCF, we employed the Bayesian Personalized Ranking (BPR) loss [30], denoted  $\mathcal{L}$ , which is frequently used in many CF methods. The BPR loss is written as follows:

$$\mathcal{L} = - \sum_{(u,i,j) \in \mathcal{B}} \ln(\sigma(\hat{r}_{ui} - \hat{r}_{uj})) + \lambda \|\Theta\|^2, \quad (3)$$

where  $\sigma$  is the sigmoid function  $\lambda$  controls the regularization term and  $\mathcal{B}$  is a mini-batch.  $\hat{r}_{ui}$  and  $\hat{r}_{uj}$  denote the predicted rating scores for a pair of positive and negative drugs of drug  $u$ . To predict  $\hat{r}_{ui}$ , we use a dot product  $\mathbf{E}_d \mathbf{E}_d^\top$ .  $\Theta$  denotes the embeddings to learn, i.e.,  $\Theta = \mathbf{E}^{(0)}$  in our DDI-OCF framework. Note that our method only learn the initial embedding. The exact training method is described in Alg. 1.

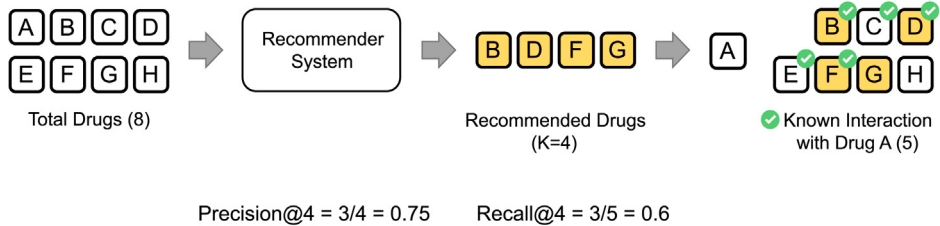


**Fig. 2.** An example of calculating a metric in a recommendation system. As shown in the figure, if there are four drugs that the model recommends as interacting with drug A, and three of them actually have an interaction (B, D, F), precision is 3 divided by 4 (the number of recommended drugs) and recall is 3 divided by 5 (the number of total known interaction with drug A).

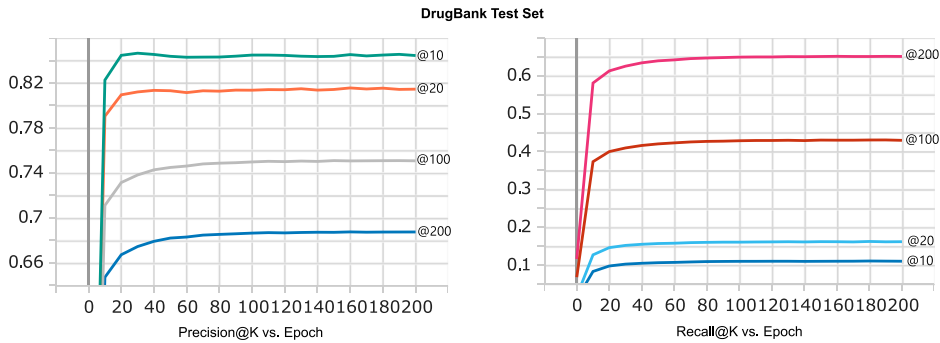


**Fig. 3.** Experimental results on DrugBank data.

---

#### Algorithm 1 How to train our proposed DDI-OCF.

---

**Require:** Interaction matrix  $A$ , Interaction score rating  $R$   
**Ensure:**  $E^{(0)}$   
 Initialize  $E^{(0)}$   
**while** the BPR loss  $\mathcal{L}$  is not converged **do**  
 Solve Eq. (1) from  $E^{(0)}$   
 Calculate the final drug embedding with Eq. (2)  
 Compute the  $\mathcal{L}$  with Eq. (3)  
 Update  $E^{(0)}$  to minimize  $\mathcal{L}$   
**end while**

---

### 3. Results and discussions

#### 3.1. Experimental evaluations

We evaluated the DDI-OCF model using DrugBank and TWOSIDES data. Table 3 reports precision and recall score for the top K recommendations. Training progressed to 200 epochs, and metrics converged to a certain value. The learning curve of the trained model can be found in Fig. 3. We conducted experiments with different values of K: 10, 20, 100 and 200. When K is set to 10, the precision@10 of the test set is 0.847. This means that on average more than 8 of the top 10 predicted interactions are indeed present in the test set. However, it should be noted that not all drugs within the test set have more than 10 interactions. Consequently, if a drug in the test set has only 5 interactions, the precision@10 for this particular drug would not exceed 0.5. On the other hand, if a considerable number of drugs possess interactions, the recall@K metric tends to yield low values. Within test set of DrugBank, the average number of edges per node is 273.4. In the case of the number of recommendations for K values of 10 or 20, the resulting recall@K will remain low, even if the ten recommendations are correct. For example, if 10 drugs are correct in a test set drug with 237 connections, the recall@10 is  $10/237 \approx 0.037$ . Fig. 4 shows a histogram of the number of edges connected for each node in the DrugBank data test set. Since there are many drugs

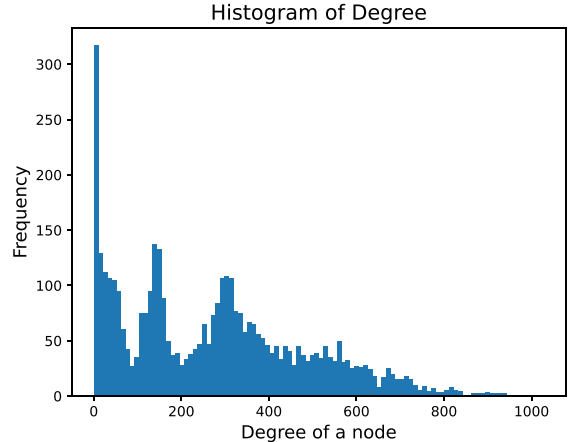


**Fig. 4.** Histogram of degree. In graph theory, the degree of a node is the number of edges connected to the node. The figure shows a histogram of the number of connected edges for each node in the test set of DrugBank data.

with an interaction of 200 or more, the corresponding recall values depicted in Table 3 is inherently low. In the DrugBank test set, there are 270 drugs with fewer than 10 interactions and 2300 drugs with more than 200 interactions. We introduced the adjusted score which can be seen in parenthetical numbers in Table 3. Among the drugs in the DrugBank test set, the average precision@10 for the 3082 drugs with at least 10 interactions is 0.881, and there are 2877 drugs with precision@10 = 1. Furthermore, the average precision@200 for the 2303 drugs with at least 200 interactions is 0.953, and there are 1033 drugs with precision@200 = 1. On the other hand, since recall@K is based on the degree of a node, the metrics calculated for drugs with K or fewer interactions are shown in parentheses in Table 3. For example, for recall@10, only 295 drugs with 10 or fewer interactions are evaluated, and the adjusted recall@10 is 0.624.

The 5-fold CV and TWOSIDES data yielded slightly lower precision and slightly higher recall than the aforementioned DrugBank results.

**Table 3**

Performance evaluation for each dataset.

Data set	DrugBank <sup>a</sup>		DrugBank 5-fold CV		TWOSIDES <sup>1</sup>	
	Precision	Recall	Precision	Recall	Precision	Recall
Top K						
Top 10	0.847 (0.881)	0.110 (0.624)	0.802 ± 0.002	0.152 ± 0.002	0.745	0.129
Top 20	0.815 (0.881)	0.162 (0.634)	0.765 ± 0.001	0.223 ± 0.001	0.707	0.230
Top 100	0.751 (0.925)	0.430 (0.725)	0.665 ± 0.002	0.610 ± 0.001	0.526	0.696
Top 200	0.688 (0.953)	0.652 (0.845)	0.525 ± 0.001	0.823 ± 0.001	0.364	0.899

The table shows the values of each metric for the test set data. The numbers in parentheses are the adjusted values, where precision@K is calculated only for drugs with K or more interactions, and recall@K is calculated only for drugs with K or fewer interactions.

<sup>a</sup> The ratio of the number of edges in the training and test sets is 6:4.

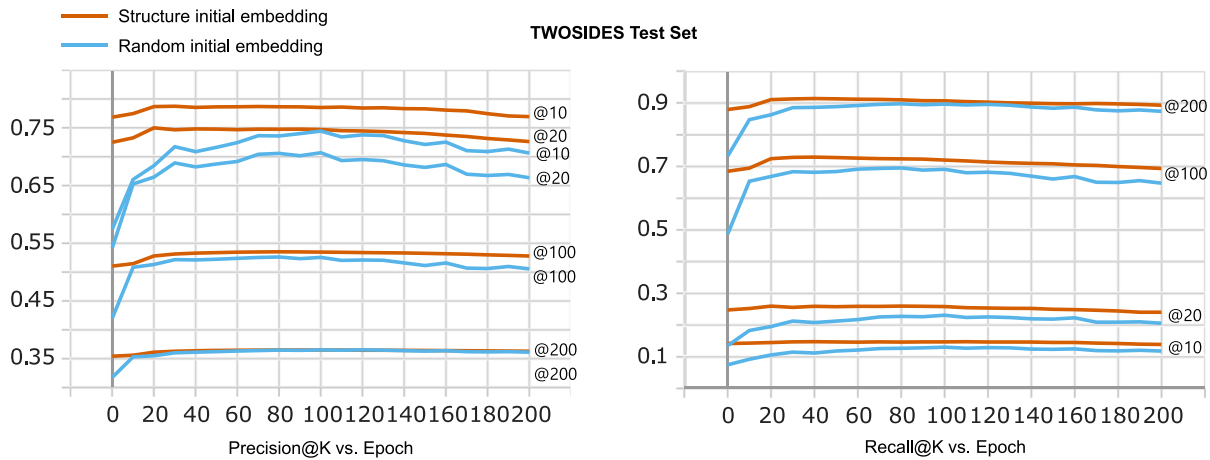


**Fig. 5.** Experimental results on TWOSIDES data. TWOSIDES is a small data set of drugs that are only small molecule. We found that the initial embedding with structure information yielded better learning results.

**Table 4**

Comparison of metrics with matrix factorization model.

Model	DDI-OCF		Matrix Factorization	
	Precision	Recall	Precision	Recall
Top K recommend				
Top 10	0.847 (0.881)	0.110 (0.624)	0.732 (0.768)	0.067 (0.385)
Top 20	0.815 (0.881)	0.162 (0.634)	0.728 (0.794)	0.112 (0.456)
Top 100	0.751 (0.925)	0.430 (0.725)	0.746 (0.922)	0.424 (0.708)
Top 200	0.688 (0.953)	0.652 (0.845)	0.690 (0.953)	0.656 (0.850)

Comparison of matrix factorization, a classical recommendation technique, and the proposed DDI-OCF using DrugBank data. The numbers in parentheses are the adjusted values.

This is also due to the smaller graph size of the test set, which means that there are fewer connections per node in the ground-truth, which explains the decrease in precision and increase in recall. The 5-fold CV results in **Table 3** consistently demonstrate minimal fluctuations up to three decimal places, indicating robustness in the face of varying data conditions.

Since TWOSIDES is a database of only small molecule drugs, we experimented with adding drug structure information. In practical experimentation, employing initial drug embeddings as structural information in the TWOSIDES data speeds up convergence early in training and increases performance, compared to not utilizing them (**Fig. 5**). We generated embedding vectors for the 645 drug structures in TWO-SIDES using a drug structure graph embedding technique pre-trained with more than 2 million compounds [31]. For a small number of recommendations, such as top10 and 20, we observed an increase in precision of about 0.04. The more recommendations the model makes, the smaller the difference in metrics. Drugs in the same class are structurally similar and can increase side effects when used together. TWOSIDES data also contain many data reporting interactions in the same family, which can be a helpful clue when trying to match a smaller number of interacting drugs. Therefore, including structural information can increase precision on fewer recommendations. Since

our goal is to identify new DDIs that are not in the same family drugs, it is encouraging to see similar scores on recall@200 (**Fig. 5**). In the Drugbank data, there are many biologics with very large and unclear chemical structures; therefore, we did not experiment with all the structures. If the training data are sufficient with a large amount, so it is expected to show no significant differences in predicting interactions for other class drugs.

In **Table 4**, we also compared our DDI-OCF model with MF [32], a classic recommendation model, and show superiority. Data are the same DrugBank used in the DDI-OCF model, and MF has lower overall scores but similar scores on top 200 recommendations. This is because we have not prioritized among DDIs; therefore, the more recommendations we generate, the higher the probability of capturing interactions in our test set. We can see from **Table 4** that there is an upward trend in adjusted score as K increases.

### 3.2. Case studies: Drugs predicted by DDI-OCF

In this section, we review the recommendations of DDI-OCF for several clinically important drugs. For illustrative purposes, we conducted comprehensive examinations of the top 10 recommendations for two drugs that exhibited fewer than 10 interactions within our test set. Additionally, we took a closer look at Humira, the top-selling drug in 2022. The evaluation of DDI-OCF was for the model trained up to the 160th epoch, which is the model with the highest precision@10.

#### 3.2.1. Oseltamivir acid

We first tried to predict interactions for oseltamivir acid, since it is one of the most famous and best-selling drugs in our test set with fewer than 10 interactions. Oseltamivir, commercially known as Tamiflu, constitutes an antiviral drug used for the treatment and prophylaxis of influenza A and influenza B. Oseltamivir acid, the active metabolite of oseltamivir phosphate, is an orally bioavailable, potent and selective inhibitor of influenza virus neuraminidase [33]. Oseltamivir acid has 7

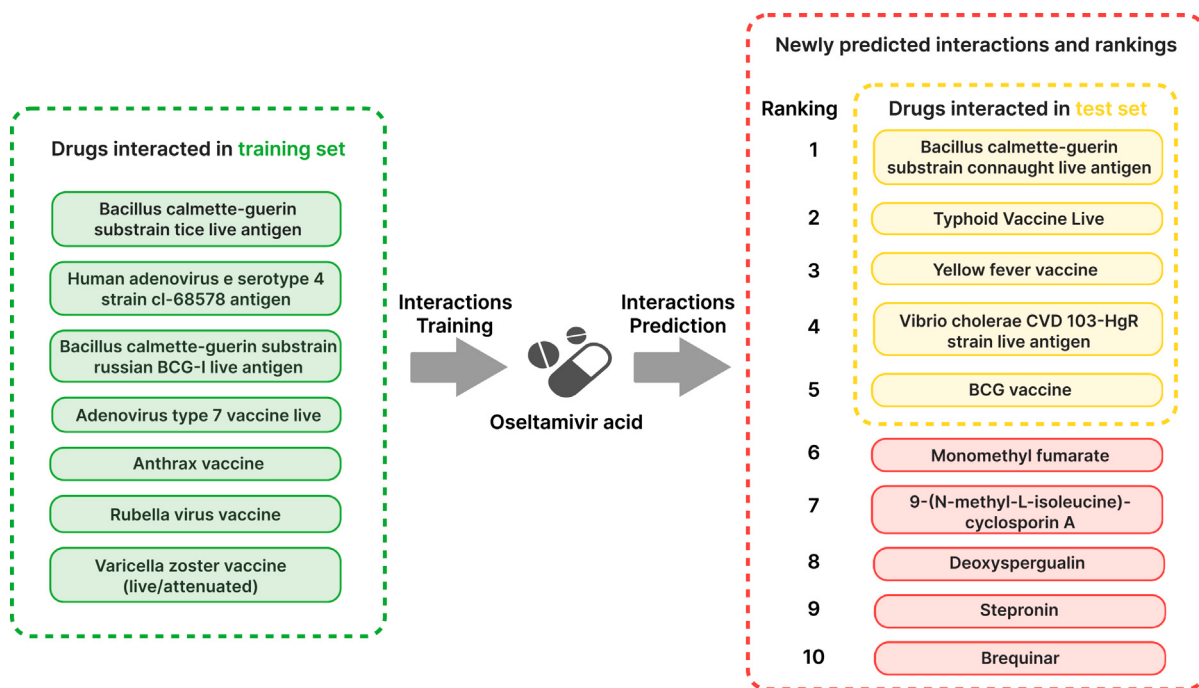


**Fig. 6.** Case study on oseltamivir acid in DrugBank dataset. DDI-OCF correctly recommends the five drugs in test set known to interact with oseltamivir acid, ranked 1 through 5, and the subsequent recommended drugs are also expected to have pharmacologically meaningful interactions. (For interpretation of the references to color in this figure legend, the reader is referred to the web version of this article.)

interactions in the training set and 5 in the test set. The seven drugs that interact with oseltamivir acid used in the training are all vaccines and viral antigens. Antivirals and antiviruses can be used in combination to have additive effect [34]. DDI-OCF recommends all five interacting vaccines present in the test set within the top 5 recommendations, although there are other vaccines or antigens in the possible choices (Fig. 6). Drugs recommended as ranked 6 through 10, indicated in the red boxes in Fig. 6 are not present in the DrugBank data. However, all of these drugs have antiviral or immunosuppressive properties that could potentially interact with antivirals such as oseltamivir. (Table 5).

Monomethyl fumarate may have addition antiviral effect when combined with oseltamivir acid. monomethyl fumarate, sold under the brand name Bafiertam, is a drug for the treatment of relapsing forms of multiple sclerosis and is available orally [35]. Dimethyl fumarate (DMF) and its active metabolite, monomethyl fumarate (MMF), are effective in the therapy of immune-mediated diseases and have potential applications to restrict the progression of HIV disease [36]. Also, DMF has been shown in a number of studies to have antiviral effects, including SARS-CoV2 [37].

9-(N-methyl-L-isoleucine)-cyclosporin A (NIM811) can help antiviral effect when combined with oseltamivir acid. NIM811 is a non-immuno-suppressive cyclosporine A analog and has been used in clinical trials investigating the treatment of chronic hepatitis C genotype-1 relapse. Recent reports suggest that cyclosporine, by binding to cellular proteins of the cyclophilin family, exhibits inhibitory effects on hepatitis C virus (HCV) replication in vitro, with compounds demonstrating a higher affinity for cyclophilin binding, such as NIM811 [38].

Deoxyspergualin can decrease the therapeutic efficacy of oseltamivir acid when used in combination with oseltamivir acid. Studies have shown that deoxyspergualin is a potent immunosuppressant with clinical potential due to its direct effects on macrophages and B cells [39]. Although direct clinical information is not available from co-administration of deoxyspergualin and oseltamivir, the use of immunosuppressive agents in antiviral therapy requires more careful dosing [40].

Strepronin may have additional antiviral effects in combination with oseltamivir acid. Streptonin is a mucolytic and an experimental

drug. It also acts as an immunosuppressant and there are studies that suggest it has antiviral property [41]. It is reasonable in a recommendation system that recommends drugs with similar mechanisms.

Brequinar is another experimental chemical exhibiting immunosuppressive activity that is considered for transplantation [42]. It was investigated in the 1990s and has not been developed, but a recent study confirmed its antiviral effects on the HIV-1 virus by in vitro cell test [43]. Although it is an experimental drug, these properties show that the drugs recommended together share a similar activity.

In subsequent rankings, we also confirmed that vaccines, immunosuppressants, and monoclonal antibody drugs dominated the recommendation rankings.

### 3.2.2. Meclocycline

Whereas meclocycline itself is not commonly used in clinical practice, it belongs to the tetracycline class of antibiotics, which finds extensive use as a first-line antibiotic for numerous infectious diseases. Meclocycline has a total of 7 interactions in our dataset, comprising 5 in the training set and 2 in the test set, allocated through a random split. The training set has estetrol, methoxyflurane, vibrio cholerae CVD 103-HgR strain live antigen, didanosine, and palovarotene. The test set has collagenase clostridium histolyticum and magnesium. All of these drugs have different mechanism of action.

DDI-OCF missed two drugs from the test set in its top 10 recommendations due to their limited interactions, hampering the learning process. Additionally, dissimilar drug characteristics between the train and test sets pose challenges for effective recommendations. The correlation between the number of interactions and learning performance is evident in the highest adjusted precision score achieved for drugs with 200 interactions.

The top 10 drugs that are suggested to have interactions with meclocycline are listed below. (1) BCG vaccine, (2) Rolitetracycline, (3) Tigecycline, (4) Lymecycline, (5) (S)-Warfarin, (6) Metacycline, (7) Ethyl biscoumacetate, (8) Oxytetracycline, (9) Clomocycline, (10) Diphenadione. Six out of ten drugs are tetracycline antibiotics. In clinical practice, duplicate prescriptions for drugs of the same class are avoided because they can increase the probability of side effects.

Therefore, the results of tetracyclines are reasonable. We investigated the interaction evidence for the remaining four drugs ([Table 6](#)).

Bacillus Calmette-Guérin (BCG) vaccine can show decreased therapeutic efficacy when used in combination with mecloxycline. The BCG vaccine is an attenuated live vaccine, and the strain, BCG, is susceptible to tetracycline class antibiotics [44,45]. Therefore, when combined with mecloxycline, an antibiotic in the tetracycline class, as it may reduce the effectiveness of the BCG vaccine. Modern medication guidelines also advise against combinations of these two drugs.

Warfarin may increase its anticoagulant activities when combined with mecloxycline. Warfarin is a vitamin K antagonist, which is a classical anticoagulant. Warfarin is a medication that must be administered closely to monitor the patient's bleeding tendencies. Tetracyclines have been observed to elevate INR via an unknown mechanism, which may potentially involve the inhibition of warfarin metabolism and plasma prothrombin activity [46–48].

Ethyl biscoumacetate is a coumarin that is used as an anticoagulant. It has actions similar to those of warfarin [49]. Therefore, interactions with tetracycline antibiotics may need to be considered in its anticoagulant action.

Diphenadione, the same vitamin K antagonist, has anticoagulant properties and serves as a rodenticide to target various rodents. As an anti-coagulant, this chemical compound exhibits an active half-life that exceeds that of warfarin and other synthetic 1,3-indandione anticoagulants [50,51].

In summary, after excluding tetracyclines, one drug is an attenuated live BCG vaccine susceptible to tetracycline antibiotics. Three drugs exhibit interactions with tetracyclines in relation to blood clotting due to sharing a mechanism of action with warfarin.

### 3.2.3. Adalimumab

We performed a prediction of the drug interactions for adalimumab. Adalimumab, a monoclonal tumor necrosis factor (TNF) alpha antibody, has application in treating a diverse range of inflammatory conditions, including rheumatoid arthritis and Crohn's disease [52,53]. The number of drugs that interact with adalimumab in the DrugBank dataset is 801 in the training set and 503 in the test set. The top 10 and top 20 recommended drugs by DDI-OCF were all drugs that were included in the test set. Also, the top 99 recommendations are all included in the test set, and the 100th recommendation is curcumin sulfate, which is not in the test set. We reviewed seven drugs that were not in the test set from DDI-OCF's top 200 recommendations for possible interactions ([Table 7](#)).

Curcumin sulfate is the sulfate salt attached to curcumin, and the pharmacological activity of curcumin is to reduce inflammation as a TNF blocker [54]. Adalimumab is also a TNF inhibitor and is used to treat inflammation, so it can be assumed that it has a similar mechanism of action.

Abiraterone can be less effective when used in combination with adalimumab. Abiraterone is a derivative of steroidial progesterone and is approved for patients with hormone refractory prostate cancer. Anti-TNF treatment can increase sex hormones [55]. TNF- $\alpha$  increases aromatase activity, which increases the conversion of androgens to estrogens in the periphery [56]. Because adalimumab inhibits TNF- $\alpha$ , inhibition of aromatase activity may be attenuated, the antiandrogenic activity of abiraterone may be interfered with. The primary pharmacological mechanism of abiraterone is to block androgen biosynthesis by inhibiting CYP17A1, which is predominantly expressed in testicular, adrenal, and prostate tissue. Furthermore, abiraterone is metabolized and inactivated by CYP3A4 [57]. Meanwhile, studies have shown that cytokines, including TNF- $\alpha$ , can inhibit CYP in hepatocytes [58,59]. In inflammatory patients receiving adalimumab, inhibition of TNF- $\alpha$  may promote CYP production, which increases abiraterone degradation by CYP3A4 and decreases CYP17A2 inhibition. Similarly, DrugBank provides information that adalimumab increases sex hormone metabolism, such as testosterone, progesterone and estrone.

Rifamycin is an antibiotic used specifically for mycobacterial diseases, including latent or active tuberculosis. A typical mycobacterial disease is tuberculosis (TB), which is caused by the mycobacterium tuberculosis. Currently, rifampicin, a more stable semi-synthetic rifamycin drug, is used for the standard treatment of mycobacterium tuberculosis. Anti-TNF therapy is recognized to increase the risk of TB. Most guidelines highly recommend stopping TNF blocker treatment for TB patients [60,61]. TNF- $\alpha$  holds an important role in granuloma formation during the anti-TB defense mechanism, and since this defense mechanism is inhibited when TNF- $\alpha$  inhibitors are administered, there is an increased risk of opportunistic diseases such as TB. Also, in non-tuberculous mycobacterial lung disease, TNF blockers can be a strong predisposing factor for infection [62]. Consequently, when considering co-administration of rifamycin and adalimumab, careful and informed decision making is imperative.

The metabolism of simeprevir can be increased when combined with adalimumab. Simeprevir is a direct-acting antiviral agent to treat chronic HCV infection. As with many antivirals, simeprevir is specifically metabolized by CYP3A4 [63]. Adalimumab is a potent TNF- $\alpha$  inhibitor, which may result in the induction of CYP, suggesting the potential for increased metabolism of simeprevir like abiraterone mentioned above [58,59]. Although adalimumab is currently not recognized as a CYP-related cautionary drug, Wen et al. demonstrated that etanercept, another TNF- $\alpha$  blocker, exerted an impact on the metabolism of cyclosporine, a substrate of CYP, by affecting CYP synthesis, resulting in a significant increase in total clearance of cyclosporine, which is at least 2.5 times [64]. Knowledge about DDIs may evolve and be revised as additional clinical data accumulate post-marketing.

The metabolism of armodafinil can be increased when combined with adalimumab. Armodafinil, an enantiomer of modafinil, functions as a stimulant to enhance wakefulness in adult patients experiencing excessive sleepiness. Although its precise mechanism of action remains unknown, it is known that glucuronide conjugation and sulfone formation by CYP 3A4/5 play the most important role in its metabolism [65]. As mentioned above, inhibition of TNF- $\alpha$  may promote the production of CYPs and thus potentially increase the metabolism of armodafinil.

The therapeutic efficacy of somapacitan can increase when used in combination with adalimumab. Somapacitan is a human growth hormone analog. There are clinical investigations indicating that anti-TNF therapies, including adalimumab, have facilitated growth in children affected by Crohn's disease [66,67]. Notably, up to 30% of pediatric patients with Crohn's disease or inflammatory bowel disease are reported to experience consistently deficit growth [68]. Inflammatory mediators impact growth by inducing growth hormone resistance. It is caused by the actions of IL-6 and TNF, which impair hepatic growth hormone signal transduction and inhibit cell proliferation at the growth plate [68].

## 4. Conclusion

We proposed DDI-OCF, a deep learning approach with GCN-based CF to predict DDIs. DDI-OCF recommend drugs that are predicted to have interactions with the drug of interest, in an orderly list. It has several advantages over classification models, including data imbalance and consequent sampling of negative samples and preprocessing of drug features such as structure and transcriptome. We embedded drug nodes using GCN with the entire DDIs network, which further improved performance by applying ODEs to achieve the effect of using continuous layers. The recommendation results using CF showed that our GCN outperformed the results of embedding with classical MF. Also, we experimented with and without structure information. It was useful to find drugs in the same class in a small number of recommendations, but for more than 100 recommendations, our model had similar predictive power without structure information. Therefore, DDI-OCF can easily predict without drug features, including not only small molecules but also biologics with large and ambiguous structure. Furthermore, our study entails a thorough examination of the model's recommendations for three drugs with significant in the pharmaceutical market, which lead to the identification of potential clinically unreported DDIs.

**Table 5**

The top 10 DDI-OCF predicted drugs for potentially interacting with Oseltamivir acid.

Rank	Candidate drugs	Interaction	Evidences
6	Monomethyl fumarate	It can have addition antiviral effect when combined with Oseltamivir acid.	[36,37]
7	NIM811	It can have addition antiviral effect when combined with Oseltamivir acid.	[38]
8	Deoxyspergualin	Deoxyspergualin can decrease the therapeutic efficacy of Oseltamivir acid.	[39,40]
9	Strepronin	It can have addition antiviral effect when combined with Oseltamivir acid.	[41]
10	Brequinar	Oseltamivir acid may require a dose adjustment when combined with Brequinar.	[42,43]

Note: The top 1–5 recommendations are drugs that already existed in the test set and were known to have interactions. There are only 5 drugs in the test set for Oseltamivir acid. Refer to Fig. 6.

**Table 6**

The top 10 DDI-OCF predicted drugs for potentially interacting with Meclocycline.

Rank	Candidate drugs	Interaction	Evidences
1	BCG vaccine	Efficacy of BCG vaccine can be decreased when combined with Meclocycline.	[44,45]
5	Warfarin	Anticoagulant effect may increase when combined with Meclocycline.	[46–48]
7	Ethyl biscoumacetate	Anticoagulant effect may increase when combined with Meclocycline.	[46,48,49]
10	Diphenadione	Anticoagulant effect may increase when combined with Meclocycline.	[46,50,51]

Note: Tigecycline, Lymecycline, Metacycline, Oxytetracycline and Clomocycline are ranked 2, 3, 4, 6, 8 and 9, respectively. They are drugs in the same tetracycline family and can have increased side effects when combined with Meclocycline.

**Table 7**

The top 10 DDI-OCF predicted drugs for potentially interacting with Adalimumab(ADA).

Rank	Candidate drugs	Interaction	Evidences
100, 154	Curcumin	Curcumin is a TNF blocker and may have addition effect with ADA.	[54]
105	Abiraterone	Abiraterone can be less effective when combined with ADA.	[57–59]
136	Rifamycin	Patients with mycobacterial disease should be cautious about using ADA.	[60–62]
172	Simeprevir	The metabolism of Simeprevir can be increased when combined with ADA.	[58,59,63]
178	Armodafinil	The metabolism of Armodafinil can be increased when combined with ADA.	[58,59,65]
198	Somapacitan	The efficacy of Somapacitan can increase when combined with ADA.	[66–68]

Note: These seven drugs are not included in the test set from the top 200 recommended drugs in the DDI-OCF.

#### 4.1. Limitation and future research

If there is a drug for which not a single interaction has been identified, it is not only difficult for the network learning, but it cannot be evaluated because it has no clinically or experimentally identified action. In this study, we use a k-core filtering ( $k = 5$ ) strategy for data quality. However, this can be unbalanced when splitting the train-test set. The density of the data used is very sparse with DrugBank at 8.39% TWOSIDES at 15.26%, which could be lower in the train-test split. Although DDI-OCF did not train about unevaluable nodes, this low-density learning performance is a result that compensates for the weaknesses of cold start. We are supplementing the training with a content base that adds transcriptome and structure information to node, and the prediction results will be evaluated by in vivo testing since there is no real world evidence. The interaction of novel targets for drugs requires the integration of diverse information such as structure, transcriptome, targets and mechanisms. Sophisticated models can utilize interaction networks with varying strengths based on evidence from the literature.

#### Key points

- Introduce a recommendation model to overcome the problem of negative samples and explore interactions in all drug combinations.
- Compared to previous DDI studies, a larger number of drugs were used as training and test data with 4072 drugs.
- Using only interaction report, we achieved similar level of evaluation metrics to those with structure information. It makes easier to analyze a large number of drugs, including biologics.

#### CRediT authorship contribution statement

**Yeon Uk Jeong:** Writing – review & editing, Writing – original draft, Visualization, Validation, Supervision, Software, Resources, Project administration, Methodology, Investigation, Formal analysis, Data curation, Conceptualization. **Jeongwhan Choi:** Supervision, Formal analysis. **Noseong Park:** Supervision. **Jae Yong Ryu:** Writing – review & editing, Supervision, Conceptualization. **Yi Rang Kim:** Writing – review & editing, Supervision, Funding acquisition.

#### Declaration of competing interest

The authors declare that they have no known competing financial interests or personal relationships that could have appeared to influence the work reported in this paper.

#### Acknowledgments

The authors thank the anonymous reviewers for their valuable suggestions. This research was supported by funds from Oncocross Co., Ltd. The research was supported by a grant (21153MFDS601) from Ministry of Food and Drug Safety in 2023.

#### Data availability

The implementation of DDI-OCF and the data preprocessing script is available at: <https://github.com/yeonuk-Jeong/DDI-OCF>.

#### References

- Hales CM, Servais J, Martin CB, Kohen D. Prescription drug use among adults aged 40–79 in the United States and Canada. 2019.
- Khorri V, Semnani S, Roshandel G. Frequency distribution of drug interactions and some of related factors in prescriptions. Med J Tabriz Univ Med Sci 2011;27(4):29–32.

- [3] Safdari R, Ferdousi R, Aziziheris K, Niakan-Kalhori SR, Omidi Y. Computerized techniques pave the way for drug-drug interaction prediction and interpretation. *BioImpacts*: BI 2016;6(2):71.
- [4] Han K, Cao P, Wang Y, Xie F, Ma J, Yu M, Wang J, Xu Y, Zhang Y, Wan J. A review of approaches for predicting drug-drug interactions based on machine learning. *Front Pharmacol* 2022;12:814858.
- [5] Vo TH, Nguyen NTK, Kha QH, Le NQK. On the road to explainable AI in drug-drug interactions prediction: A systematic review. *Comput Struct Biotechnol J* 2022;20:2112–23.
- [6] Li P, Huang C, Fu Y, Wang J, Wu Z, Ru J, Zheng C, Guo Z, Chen X, Zhou W, et al. Large-scale exploration and analysis of drug combinations. *Bioinform* 2015;31(12):2007–16.
- [7] Ryu JY, Kim HU, Lee SY. Deep learning improves prediction of drug-drug and drug-food interactions. *Proc Natl Acad Sci* 2018;115(18):E4304–11.
- [8] Dang LH, Dung NT, Quang LX, Hung LQ, Le NH, Le NTN, Diem NT, Nga NTT, Hung S-H, Le NQK. Machine learning-based prediction of drug-drug interactions for histamine antagonist using hybrid chemical features. *Cells* 2021;10(11):3092.
- [9] Yan X-Y, Yin P-W, Wu X-M, Han J-X. Prediction of the drug-drug interaction types with the unified embedding features from drug similarity networks. *Front Pharmacol* 2021;12:794205.
- [10] Patrick MT, Bardhi R, Raja K, He K, Tsai LC. Advancement in predicting interactions between drugs used to treat psoriasis and its comorbidities by integrating molecular and clinical resources. *J Am Med Inform Assoc* 2021;28(6):1159–67.
- [11] Kim E, Nam H. DeSIDE-DDI: interpretable prediction of drug-drug interactions using drug-induced gene expressions. *J Cheminformatics* 2022;14(1):1–12.
- [12] Zhang W, Chen Y, Li D, Yue X. Manifold regularized matrix factorization for drug-drug interaction prediction. *J Biomed Inform* 2018;88:90–7.
- [13] Shtrat G, Rokach L, Shapira B. Detecting drug-drug interactions using artificial neural networks and classic graph similarity measures. *PloS One* 2019;14(8):e0219796.
- [14] Rohani N, Eslahchi C, Katanforoush A. Iscmf: Integrated similarity-constrained matrix factorization for drug-drug interaction prediction. *Netw Model Anal Heal Inform Bioinform* 2020;9:1–8.
- [15] Zitnik M, Agrawal M, Leskovec J. Modeling polypharmacy side effects with graph convolutional networks. *Bioinform* 2018;34(13):i457–66.
- [16] Feng Y-H, Zhang S-W, Shi J-Y. Dpddi: a deep predictor for drug-drug interactions. *BMC Bioinformatics* 2020;21(1):1–15.
- [17] Feng Y-H, Zhang S-W, Shi J-Y. Dpddi: a deep predictor for drug-drug interactions. *BMC Bioinformatics* 2020;21(1):1–15.
- [18] Lin J, Wu L, Zhu J, Liang X, Xia Y, Xie S, Qin T, Liu T-Y. R2-DDI: relation-aware feature refinement for drug-drug interaction prediction. *Brief Bioinform* 2023;24(1):bbac576.
- [19] Nyamabo AK, Yu H, Shi J-Y. SSI-DDI: substructure–substructure interactions for drug–drug interaction prediction. *Brief Bioinform* 2021;22(6):bbab133.
- [20] Dewulf P, Stock M, De Baets B. Cold-start problems in data-driven prediction of drug–drug interaction effects. *Pharmaceutics* 2021;14(5):429.
- [21] Yu H, Li K, Dong W, Song S, Gao C, Shi J. Attention-based cross domain graph neural network for prediction of drug–drug interactions. *Brief Bioinform* 2023;bbad155.
- [22] Su X, You Z, Huang D, Wang L, Wong L, Ji B, Zhao B. Biomedical knowledge graph embedding with capsule network for multi-label drug–drug interaction prediction. *IEEE Trans Knowl Data Eng* 2022;35(6):5640–51.
- [23] Wishart DS, Feunang YD, Guo AC, Lo EJ, Marcu A, Grant JR, Sajed T, Johnson D, Li C, Sayeeda Z, et al. DrugBank 5.0: a major update to the DrugBank database for 2018. *Nucleic Acids Res* 2018;46(D1):D1074–82.
- [24] Zitnik M, Sosic R, Leskovec J. BioSNAP datasets: Stanford biomedical network dataset collection. 2018;5(1). Note: <http://snap.stanford.edu/biodata>.
- [25] Choi J, Jeon J, Park N. Lt-ofc: Learnable-time ocf-based collaborative filtering. In: Proceedings of the 30th ACM international conference on information & knowledge management. 2021, p. 251–60.
- [26] He X, Deng K, Wang X, Li Y, Zhang Y, Wang M. LightGCN: Simplifying and powering graph convolution network for recommendation. In: SIGIR. 2020.
- [27] Chen RT, Rubanova Y, Bettencourt J, Duvenaud DK. Neural ordinary differential equations. *Adv Neural Inf Process Syst* 2018;31.
- [28] Lu Y, Zhong A, Li Q, Dong B. Beyond finite layer neural networks: Bridging deep architectures and numerical differential equations. In: International conference on machine learning. PMLR; 2018, p. 3276–85.
- [29] Lu Y, Zhong A, Li Q, Dong B. Beyond finite layer neural networks: Bridging deep architectures and numerical differential equations. In: International conference on machine learning. PMLR; 2018, p. 3276–85.
- [30] Rendle S, Freudenthaler C, Gantner Z, Schmidt-Thieme L. BPR: Bayesian personalized ranking from implicit feedback. In: UAI. 2009.
- [31] Hu W, Liu B, Gomes J, Zitnik M, Liang P, Pande V, Leskovec J. Strategies for pre-training graph neural networks. 2019, arXiv preprint arXiv:1905.12265.
- [32] Koren RB, Volinsky C. Matrix factorization techniques for recommender systems. *Comput* 2009;42(8):30–7.
- [33] Li W, Escarpe PA, Eisenberg EJ, Cundy KC, Sweet C, Jakeman KJ, Merson J, Lew W, Williams M, Zhang L, et al. Identification of GS 4104 as an orally bioavailable prodrug of the influenza virus neuraminidase inhibitor GS 4071. *Antimicrob Agents Chemother* 1998;42(3):647–53.
- [34] Godoy P, Soldevila N, Martínez A, Godoy S, Jané M, Torner N, Acosta L, Rius C, Domínguez À, of Hospitalized Cases of Severe Influenza in Catalonia Working Group S. Effectiveness of influenza vaccination and early antiviral treatment in reducing pneumonia risk in severe influenza cases. *Vaccines* 2024;12(2):173.
- [35] DailyMed. Bafertam- monomethyl fumarate capsule. URL <https://dailymed.nlm.nih.gov/dailymed/drugInfo.cfm?setid=a161f9d4-70f1-4097-957a-eafb35d3274f>.
- [36] Gill AJ, Kolson DL. Dimethyl fumarate modulation of immune and antioxidant responses: application to HIV therapy. *Crit Rev™ Immunol* 2013;33(4).
- [37] Olagnier D, Farahani E, Thyrsted J, Blay-Cadanet J, Herengt A, Idorn M, Hait A, Hernaez B, Knudsen A, Iversen MB, et al. SARS-CoV2-mediated suppression of NRF2-signaling reveals potent antiviral and anti-inflammatory activity of 4-octyl-itaconate and dimethyl fumarate. *Nat Commun* 2020;11(1):4938.
- [38] Ma S, Boerner JE, TiongYip C, Weidmann B, Ryder NS, Cooreman MP, Lin K. NIM811, a cyclophilin inhibitor, exhibits potent in vitro activity against hepatitis C virus alone or in combination with alpha interferon. *Antimicrob Agents Chemother* 2006;50(9):2976–82.
- [39] Thomas FT, Tepper MA, Thomas JM, Haisch CE. 15-Deoxyspergualin: a novel immunosuppressive drug with clinical potential. *Ann New York Acad Sci* 1993;685:175–92.
- [40] Lemaitre F, Budde K, Van Gelder T, Bergan S, Lawson R, Noceti O, Venkataraman R, Elens L, Moes DJA, Hesselink DA, et al. Therapeutic drug monitoring and dosage adjustments of immunosuppressive drugs when combined with nirmatrelvir/ritonavir in patients with COVID-19. *Ther Drug Monit* 2022;10:1097.
- [41] de Giorgi L, Habeshaw J, Broadhurst K, Carminati P, Oxford J. Anti-human immunodeficiency virus activity of a new immunosuppressant drug called stepronin. In: *Transplantation proceedings*. vol. 31, 1999, 3257–3257.
- [42] Makowka L, Sher LS, Cramer DV. The development of Brequinar as an immunosuppressive drug for transplantation. *Immunol Rev* 1993;136:51–70.
- [43] Andersen PL, Krpina K, Janevski A, Shtaida N, Jo E, Yang J, Koit S, Tenson T, Hukkanen V, Anthonsen MW, et al. Novel antiviral activities of obatoclax, emetine, niclosamide, brequinar, and homoharringtonine. *Viruses* 2019;11(10):964.
- [44] Durek C, Rüsch-Gerdes S, Jocham D, Böhle A. Sensitivity of BCG to modern antibiotics. *Eur Urol* 1999;37(Suppl. 1):21–5.
- [45] Ramón-García S, Mick V, Daïne E, Martín C, Thompson CJ, De Rossi E, Manganello R, Alins JA. Functional and genetic characterization of the tap efflux pump in *Mycobacterium bovis* BCG. *Antimicrob Agents Chemother* 2012;56(4):2074–83.
- [46] Seamans E. Antibiotic and anticoagulation: watching warfarin levels. In: *The neuriva brain health challenge* is sponsored by RB Health. Also, (Azithromycin [prescribing information]. New York, NY: Pfizer Labs; 2017.
- [47] Hasan SA. Interaction of doxycycline and warfarin: an enhanced anticoagulant effect. *Cornea* 2007;26(6):742–3.
- [48] Rice P, Perry R, Afzal Z, Stockley I. Antibacterial prescribing and warfarin: a review. *Br Dent J* 2003;194(8):411–5.
- [49] Martindale W. *The extra pharmacopoeia* 30th ed. 1993, p. 226.
- [50] Meister RT. *Farm chemicals handbook'*92. 1992.
- [51] Griffin JP, D'Arcy PF. *A manual of adverse drug interactions*. Elsevier; 1997.
- [52] Kitzvitz A, Segurado OG. HUMIRA® pen: a novel autoinjection device for subcutaneous injection of the fully human monoclonal antibody adalimumab. *Expert Rev Med Devices* 2007;4(2):109–16.
- [53] Scheinfeld N. Adalimumab (HUMIRA): a review. *J Drugs Dermatol: JDD* 2003;2(4):375–7.
- [54] Aggarwal BB, Gupta SC, Sung B. Curcumin: an orally bioavailable blocker of TNF and other pro-inflammatory biomarkers. *Br J Pharmacol* 2013;169(8):1672–92.
- [55] DeBoer MD, Thayu M, Griffin LM, Baldassano RN, Denson LA, Zemel BS, Denburg MR, Agard HE, Herskovitz R, Long J, et al. Increases in sex hormones during anti-tumor necrosis factor  $\alpha$  therapy in adolescents with Crohn's disease. *J Pediatr* 2016;171:146–52.
- [56] Cutolo M, Sulli A, Capellino S, Villaggio B, Montagna P, Pizzorni C, Paolino S, Seriolo B, Felli L, Straub RH. Anti-TNF and sex hormones. *Ann New York Acad Sci* 2006;1069(1):391–400.
- [57] Bernard A, Vaccaro N, Acharya M, Jiao J, Monbalu J, De Vries R, Stieljes H, Yu M, Tran N, Chien C. Impact on abiraterone pharmacokinetics and safety: Open-label drug–drug interaction studies with ketoconazole and rifampicin. *Clin Pharmacol Drug Dev* 2015;4(1):63–73.
- [58] Abdel-Razzak Z, Loyer P, Fautrel A, Gautier J-C, Corcos I, Turlin B, Beaune P, Guillouzo A. Cytokines down-regulate expression of major cytochrome P-450 enzymes in adult human hepatocytes in primary culture. *Mol Pharmacol* 1993;44(4):707–15.
- [59] Stipp MC, Acco A. Involvement of cytochrome P450 enzymes in inflammation and cancer: a review. *Cancer Chemother Pharmacol* 2021;87(3):295–309.
- [60] Wallis RS. Tumour necrosis factor antagonists: structure, function, and tuberculosis risks. *Lancet Infect Dis* 2008;8(10):601–11.
- [61] Dixon W, Hyrich K, Watson K, Lunt M, Galloway J, Ustianowski A, Symmons D, Consortium BCC, et al. Drug-specific risk of tuberculosis in patients with rheumatoid arthritis treated with anti-TNF therapy: results from the British Society for Rheumatology Biologics Register (BSRBR). *Ann Rheum Dis* 2010;69(3):522–8.

- [62] Aksamit TR, Philley JV, Griffith DE. Nontuberculous mycobacterial (NTM) lung disease: the top ten essentials. *Respir Med* 2014;108(3):417–25.
- [63] Talavera Pons S, Boyer A, Lamblin G, Chennell P, Châtenet F-T, Nicolas C, Sautou V, Abergel A. Managing drug-drug interactions with new direct-acting antiviral agents in chronic hepatitis C. *Br J Clin Pharmacol* 2017;83(2):269–93.
- [64] Wen H, Chen D, Lu J, Jiao Z, Chen B, Zhang B, Ye C, Liu L. Probable drug interaction between etanercept and cyclosporine resulting in clinically unexpected low trough concentrations: first case report. *Front Pharmacol* 2020;11:939.
- [65] Garnock-Jones KP, Dhillon S, Scott LJ. Armofitinil. *CNS Drugs* 2009;23:793–803.
- [66] Malik S, Ahmed S, Wilson M, Shah N, Loganathan S, Naik S, Bourke B, Thomas A, Akobeng A, Fagbemi A, et al. The effects of anti-TNF- $\alpha$  treatment with adalimumab on growth in children with Crohn's disease (CD). *J Crohn's Colitis* 2012;6(3):337–44.
- [67] Assa A, Hartman C, Weiss B, Broide E, Rosenbach Y, Zevit N, Bujanover Y, Shamir R. Long-term outcome of tumor necrosis factor alpha antagonist's treatment in pediatric Crohn's disease. *J Crohn's Colitis* 2013;7(5):369–76.
- [68] Sanderson IR. Growth problems in children with IBD. *Nat Rev Gastroenterol Hepatol* 2014;11(10):601–10.